Journal of Applied Polymer Science

REVIEW

Contact Mechanics and Tribology of Polymer Composites

Nikolai Myshkin,[1] Alexander Kovalev,[2] Dirk Spaltman,[2] Mathias Woydt[2]

[1]Metal-Polymer Research Institute of Belarus National Academy of Sciences (MPRI), Kirov Str. 32A, 246050 Gomel, Belarus

[2]Federal Institute for Materials Research and Testing (BAM), Unter den Eichen 87, 12205 Berlin, Germany

Correspondence to: A. Kovalev (E-mail: alexander.kovalev@bam.de)

ABSTRACT: We review contact mechanics with emphasis on the rheological (time dependent) properties of polymers and their relations to surface roughness, material properties, and friction as well as wear behavior of rubbing polymer surfaces. The main concept of polymer mechanics related to tribology consists of three basic elements involved in friction: deformation resulting in the real area of contact of rough surfaces, contact adhesion, and shear and rupture of materials in the contact during the sliding friction. The results of classical work are included, which addresses the real contact area calculation and the description of adhesion interaction between rough surfaces. A brief review of experimental investigations concerning the surface characterization by means of bearing curves, the intermolecular force interaction using the adhesion parameter, the effect of temperature on the real contact area, the formation of transferred polymer film during friction, and tribological behavior of ultrathin polymer layers are presented and their implications discussed. © 2013 Wiley Periodicals, Inc. J. Appl. Polym. Sci. **2014**, *131*, 39870.

KEYWORDS: surfaces and interfaces; friction; wear and lubrication; mechanical properties; microscopy; properties and characterization

Received 21 May 2013; accepted 15 August 2013

DOI: 10.1002/app.39870

INTRODUCTION

There are three important factors affecting friction: deformation affecting the real area of contact of surfaces, adhesion of surfaces in contact, and also shear resulting in film transfer and debris formation.[1,2] The deformation component of friction results from the resistance of the polymer to "ploughing" by the asperities of the harder counterface. Polymer surface asperities experience elastic, plastic, and viscoelastic deformation depending on the material properties. The adhesion component stems from the adhesive junctions formed on the spots of real contact between the mated surfaces. The adhesion component of friction for polymers is believed to exceed by far the deformation. Special consideration is needed for transfer films, being the key factor, which determine the tribological behavior of polymers and polymer composites.[1–5]

It is known that the size of linear macromolecules of polymers is very big and the main feature of the polymer structure is that macromolecules consist of the rigid segments which can rotate, thus providing the flexibility of the molecular chains. Another feature of polymers is that strong chemical forces link the atoms in a polymer chain, whereas the intermolecular forces, which are significantly weaker, link the chains. The structural features of polymers and the possibility of changing their properties within a wide range provide a variety of the tribological applications of polymers and polymer composites.

The application of the different fillers gives an opportunity of improving the tribological behavior of polymers.[6–8] For example, the reinforcement with short fibers (glass or carbon) is used most often to increase the mechanical strength, hence, the load-bearing capacity of polymer composites. Solid lubricants such as polytetrafluoroethylene (PTFE), graphite, molybdenum disulphide added to polymers affect significantly the formation of the transfer films on the counterface and decrease the friction coefficient.[9,10] In recent years, owing to rapid advances in nanotechnologies, polymer nanocomposites being a polymer matrix filled with the particles 100 nm and smaller in size, have become more and more common.[11,12] Commonly used nanofillers in plastics are the carbon materials (fullerene and its derivatives), layered clayey minerals, and nanoparticles of metals or their organic and inorganic compounds.

Temperature affects essentially the molecular-kinetic processes proceeding in polymers and their mechanical behavior including tribological properties.[10,13,14] As experiments have shown, there exists certain equivalence between the time effect and the temperature effect on mechanical behavior of polymers. A temperature rise produces such an effect as if the process accelerates. That is, the time scale of a given viscoelastic measurement can be significantly extended, and the experiments can be conducted by the shortcut methods. This finding lent impetus to extensive studies of temperature effect on viscoelastic properties of

polymers dealing with the time-temperature superposition.[4,15] In a case of reinforced polymers by fillers, the wear behavior can be significantly different to the unfilled polymers. For example, due to an improper adhesion interaction between fillers and polymer matrix, wear volume of thermoplastic polyurethane was significantly higher than those for the unfilled polyurethane.[16]

The phenomenon of friction transfer is observed for nearly all materials. The consequences of material transfer may be significantly distinct.[17–19] If the small particles of micrometer size are transferred from one surface to the other the wear rate varies only slightly.[20] Under certain conditions the situations take place such that a thin film of the soft material is transferred onto the hard mating surface, for example, polymer on metal. If the transferred polymer film is carried away from the steel surface and is continuously formed the wear rate increases. In the case when the film is held in place, the friction occurs between the similar materials which may eventually result in seizure. Spreading of the polymer on steel gives rise to an abrupt jump of the friction force, but the wear changes insignificantly.

The unique ultrathin polymer layers[21–23] architecture with the presence of active functional groups make polymer molecules a versatile tool for modifying surface interfaces at nanolevel. Several different sets of polymers and polyions can be chosen as possible substances for deposition onto the surface: polyheteroarylenes, and their complexes with stearic acid (NBI and NBI-St), polyester acid-poly[2,4,7-trioxaheptylpyromellitic acid] (PTA), oligo- and poly(acrylic acid) (PAA), polymethylacrylate (PMA), poly(styrene-*co*−2,3,4,5,6-pentafluorostyrene) (PSF), polystyrene (PS), perfluoropolyether (PFPE), polybutylacrylate (PBA), and poly(1,6-hexanediol dimethacrylate) (PHDM) to name but a few.

Densely grafted polymer molecules tend to stretch away from the surface to reduce their interaction with other molecules, thus attaining a different conformation than the optimal for the free polymer molecules in the bulk or solution. Typically, polymer brushes synthesized by physisorption consist of two-component polymer chains, where one part strongly adheres to the interface and the second part extends to generate the polymer nanolayer. This tethering point can be a single point, in the case of a functionalized polymer chain, or some limited area as in a diblock copolymer chain. Ultrathin polymer brush layers can significantly affect surface properties of the substrates such as adhesion, lubrication, wettability, friction, and biocompatibility.

THEORETICAL SECTION

General Viscoelastic Strain–Stress Relation

The mechanical behavior of polymers is governed by the combination of elasticity and viscosity. At small deformation, polymers behave as the Hook elastic body ($\sigma = E\varepsilon$, where σ and ε are the stress and strain, and E is the modulus of elasticity) modeled with a spring and Newtonian fluid ($\sigma = \eta d\varepsilon/dt$, where η is the viscosity and t is the time); the latter is presented by a damper. The combination of these elements gives simple models of viscoelastic contact. These models allow to qualitatively estimate how polymers behave in certain situations. In more general form, the constitutive law is written as an ordinary differential equation with constant coefficients:

$$a_0\sigma + a_1\frac{d\sigma}{dt} + \ldots + a_m\frac{d^m\sigma}{dt^m} = b_0\varepsilon + b_1\frac{d\varepsilon}{dt} + \ldots + b_n\frac{d^n\varepsilon}{dt^n} \qquad (1)$$

where $a_0,\ldots, a_m$, $b_0,\ldots, b_n$ are the constant coefficients governing the mechanical behavior of the polymer under study.

For the combined stress–strain state described by tensors σ_{ij} and ε_{ij}, the above constitutive law is

$$P_1(D)s_{ij} = Q_1(D)e_{ij}$$
$$P_2(D)\sigma_{ij} = Q_2(D)\varepsilon_{ij}$$

where P_m, Q_m ($m = 1, 2$) are operator polynomials of the partial derivative with respect to time ($D = \partial/\partial t$), σ_{ij} and ε_{ij} are the stress and strain tensors, s_{ij} and e_{ij} are deviator components defined as $s_{ij} = \sigma_{ij} - \sigma_{kk}\delta_{ij}/3$, $e_{ij} = \varepsilon_{ij} - \varepsilon_{kk}\delta_{ij}/3$.

Such representation is a set of relaxation (retardation) times, which enable the relaxation (creep) curves to be described as a finite series of exponents. What actually happens is that the relaxation (retardation) times are fitted to the measured curves of relaxation (or creep). As a result, a discrete spectrum of relaxation times is found.

However, every so often, the polymer behavior cannot be described by a set of exponents. In this case the stress–strain relationship is specified in the integral form. It is assumed that there exists a continuous spectrum of relaxation times:

$$s_{ij}(x,t) = \int_{-\infty}^{t} G(t-t')\frac{\partial e_{ij}(x,t')}{\partial t'}dt', \qquad (2)$$

where G is the relaxation modulus.

Contact Mechanics of Bodies

Consider basics of contact mechanics useful for explanation of polymer contact and tribological behavior.[24] The real and nominal contact areas are determined based on solutions to the problems of the theory of viscoelasticity and elasticity.

It is known, that the contact problem on penetration of rigid ball into elastic half-space is reduced to solution of the integral equation:

$$\frac{1}{\pi}\int\int_A E'\frac{p(x',y')dA'}{\rho} = \delta - \frac{x^2}{2R} - \frac{y^2}{2R} \qquad (3)$$

where $E' = \frac{3K-4G}{6K+2G}\frac{1}{2G}$, $\rho = \left[(x-x')^2 + (y-y')2\right]^{1/2}$, K and G are bulk and shear moduli, R is the radius of rigid ball, and δ is displacement of surface.

In the case of viscoelastic behavior of bodies, the moduli entering eq. (3) are time-dependent functions and the contact area A varies in time. A viscoelastic analogue of eq. (3) is written as

$$\frac{1}{\pi}\int\int_{A(t)} E^*\frac{p(x',y')dA'}{\rho} = \delta(t) - \frac{x^2}{2R} - \frac{x^2}{2R}, \qquad (4)$$

where * stands for convolution and the function E' is determined from the integral equation:

$$2G^*(6K+2G)^*E = 3K + 4G. \qquad (5)$$

Solution of last equation for the case of constant load w gives the relation for the contact radius:

$$a^3(t)=\frac{3}{4}wRE'(t)$$

and thereby the contact area is

$$A_c=\pi\left(\frac{3}{4}wRE'(t)\right)^{2/3}$$

The use of the relations obtained depends on the choice of the constitutive law of the hereditary type. In particular, in case a material has a time-independent Poisson's ratio and kernel of heredity of the exponential type $R(t)=\frac{1}{\tau}\exp(-1/\tau)$, a time-dependent elasticity is:

$$E'(t)=\frac{1-\nu^2}{E}\frac{1}{1-\lambda}\left[1-\lambda\exp\left(-\frac{1-\lambda}{\tau}t\right)\right], \quad (6)$$

and then

$$A_c=\pi\left[\frac{3}{4}NR\frac{1-\nu^2}{E}\frac{1}{1-\lambda}\left[1-\lambda\exp\left(-\frac{1-\lambda}{\tau}t\right)\right]\right]^{2/3}. \quad (7)$$

Contact Problems with Adhesion Interaction

The work of adhesion interaction between Solids 1 and 2, equal to the work of adhesion rupture, is determined by the Dupre formula $\gamma=\gamma_1+\gamma_2-\gamma_{12}$, where γ_1 and γ_2 are the energies required to form the unit surfaces of Solids 1 and 2 (their free surface energy) and γ_{12} is the excessive or interphase energy.

Several models have been developed to describe the contact adhesion. The Johnson-Kendall-Roberts (JKR) model[25] sometimes referred to as the model of contact mechanics and the Derjaguin–Muller–Toporov (DMT) model[26] are commonly used.

The JKR model is based on the assumption on an infinitely small radius of effect of surface forces, i.e., it is assumed that interactions occur only within the contact area. Elastic contact between a sphere of radius R and half-space is analyzed with consideration of van der Waals forces which compress the mated bodies together in addition to the load applied. The contact stiffness resists to the action of the forces.

The formula for calculating the radius of JKR's adhesive contact is

$$a^3=\frac{3}{4}\frac{R}{E^*}\left(w+3\pi R\gamma+\sqrt{6\pi Rw\gamma+(3\pi R\gamma)^2}\right), \quad (8)$$

where w is the normal load.

Therefore, it is apparent that without adhesion ($\gamma=0$) the Hertz equation is obtained while if $\gamma>0$ the contact area always exceeds that of the Hertzian contact area under the same normal load w.

Only the application of a tensile (negative) load can reduce this radius, and then the contacting surfaces would separate at the least load corresponding to the conversion of the radicand into zero

$$F_{\text{pull}-\text{off}}=-\frac{3}{2}\pi R\gamma. \quad (9)$$

This circumstance is the specific feature of the JKR model.

The DMT model describes the contact of an elastic sphere with a rigid half-space. This model is based on the following two postulates: surface forces do not change the deformed profile of the sphere and it remains Hertzian; the attraction force acts outside the contact circle pressing the bodies together with the contact region being under compression by the stresses distributed according to Hertz.

Equilibrium is reached, if the deformation is sufficient for the elastic response (the force of elastic restoration of the sphere) F_e to counterbalance the joint effect of the applied external load w and the forces of molecular attraction F_s:

$$F_e=w+F_s. \quad (10)$$

In this case, the attraction is represented by the Lennard–Jones potential. Then the molecular attraction force is calculated by the direct integration:

$$F_s=2\pi\int_a^\infty p(h+h_0)rdr, \quad (11)$$

where h_0 is the equilibrium state (the clearance within the contact site).

The calculation of this integral is rather difficult yet a number of approximate formulas are known which facilitate the use of the model in question. In particular, there is a simple relation between the load and approach obtained for the conditions of the DMT model:

$$\frac{w}{F_c}=\frac{1}{\sqrt{3}}\left(\frac{\delta}{\delta_c}\right)^{3/2}-\frac{4}{3}, \quad (12)$$

where δ is elastic displacement, $F_c=\frac{3}{2}\pi\gamma R$, $\delta_c=\left(\frac{F_c^2}{3E^2R}\right)^{1/3}$.

Characterization of Rough Surfaces

A study of bearing area curve (or so-called Abbott–Firestone curve[27]) allows the display of statistical cumulative distribution of height points of a profile or surface. This cumulative distribution of height points is the basis for some roughness parameters defined in national and international standards DIN 4776[28] and ISO 13565.[29] The main weaknesses of the statistical cumulative distribution of height points (Abbott–Firestone curve) for estimating tribological behavior of surface are

1. Abbott–Firestone curve does not contain information on spatial features of the surfaces,
2. actually none of the statistical parameters of a surface heights (such as Ra, Rq, Rsk, Rku, Rpk, Rsk, and so on) are indicative for the contact or friction and wear problems allowing to calculate the important tribological characteristics of rubbing surfaces[30] (such as: real contact area (RCA), local pressure on the contact spots, coefficient of friction, wear rate and etc.).

Usually, the probability distribution of height points is determined using measurement data and/or theories of roughness. The typical way of specifying surface roughness for tribological studies is estimating the height (amplitude) statistical parameters, such as arithmetic average height (Ra), root mean square roughness (Rq), skewness (Rsk), kurtosis (Rku), and others which are mainly corresponding to the features of height points density (see Figure 1).[29–31] For surface characterization the letter "S" is used for amplitude statistical parameters instead "R" for

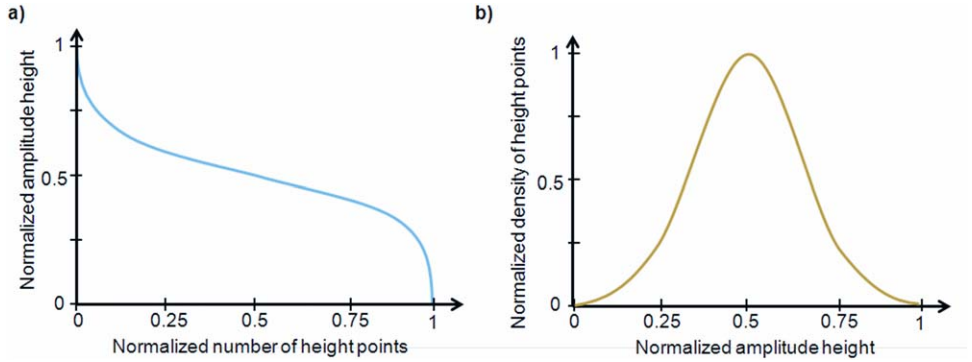

Figure 1. General statistical curves are utilized for surface characterization in tribology. (a) Cumulative distribution of height points (Abbott–Firestone curve[27]). (b) Density distribution of height points (Gaussian density curve). [Color figure can be viewed in the online issue, which is available at wileyonlinelibrary.com.]

profile characterization.[31–33] Here are the main features of the height (amplitude) statistical parameters briefly discussed. Ra (Sa) parameter is defined as the average deviation of the roughness irregularities from the mean line over sampling length, or from a mean surface over the area of nominal surface in case of areal characterization. In most of the cases this roughness parameter is used for general control of surface quality. This parameter corresponds to the maximum of density distribution shown in Figure 1(a). The main weakness is that Ra (Sa) has not any information about the profile shape or texture of surface and it is not sensitive to the fine changes of asperities peaks and deepness of pits. Rq (Sq) parameter is the standard deviation of the distribution of profile or surface height points. This parameter is sensitive to the changes of height amplitude of profile (or surface) because of the width of "bell curve" is changed in this case. Rsk (Ssk) qualifies the symmetry of the height distribution about the mean line for a profile or mean plane in a case of a surface. Mathematically this parameter describes the shape of the height distribution curve. For the Gaussian distribution, which has a symmetrical "bell-like" shape of distribution, the Rsk (Ssk) is zero. For asymmetric distribution of profile/surface heights, the Ssk may be negative or positive. It is believed that Rsk (Ssk) is the positive in case a surface has a lot of peaks and small amount of valleys, but the negative Ssk indicates that the quantity or deepness of valleys dominate the peaks above the mean plane. Kku (Sku) qualifies the flatness of the height distribution curve. The profile or surface with a Gaussian distribution of height points has a kurtosis value of 3. Centrally distributed surfaces have a kurtosis value larger than 3, whereas the kurtosis of a well spread distribution is smaller than 3.

Actually, the statistical roughness parameters of height points of rough surfaces have no direct relation to the functional properties of surfaces, however the correlation between tribological behavior of surface and the changes of their roughness parameters were found and discussed quite some time ago.[34–38] These statistical parameters describe the shape and location of derivative's extreme points on the density height (amplitude) curve. Perhaps, Thomas[36] was the first who noted that statistical roughness parameters cannot correctly describe the real surface topography. Furthermore, absolutely different surface topographies can lead to the same roughness parameters.[39] Up to day, no single approach to the problem provides a complete description of the surface topography depends on the changes on the polymer surface structure due to friction.

Contact of Rough Polymer Surfaces

When two surfaces approach each other, their opposing asperities with maximum heights come into contact forming the individual spots. The total area of these spots is known as the RCA. When estimating the real contact in the case of plastics during friction, the temperature and sliding velocity should be taken into account.[40–42]

The solution desired, i.e., the relationship between the total load w, circular contact radius a, and approach of the sphere δ is sought as a superposition of the solutions for the problems considering mechanical loading and heating. It is possible to find the total area of all contact spots (RCA) and the total load following the Greenwood-Williamson approach.[43] The nondimensional equations for the normal distribution of the asperity heights are written as follows:

$$A_r/A_a = \pi R D \sigma_r \frac{1}{\sqrt{2\pi}} \int_h^\infty (\xi - h) \exp\left[-\xi^2/2\right] d\xi, \tag{13}$$

$$\frac{w}{A_a}\frac{(1-\nu^2)}{E} = \frac{4}{3} R^{1/2} D \sigma_r^{3/2} \frac{1}{\sqrt{2\,\pi}} \int_h^\infty (\xi - h)^{3/2} \exp\left[-\xi^2/2\right] d\xi + + \frac{2\,\alpha\,T}{\pi}(1+\nu) R D \sigma_r \frac{1}{\sqrt{2\,\pi}} \int_h^\infty (\xi - h) \exp\left[-\xi^2/2\right] d\xi. \tag{14}$$

Here A_a is the apparent contact area, A_r is the RCA, D is the surface density of asperities, σ_r is the root- mean -square roughness, α is the bandwidth parameter, ξ is the nondimensional height of asperity, and h is the nondimensional separation.

It is known that the RCA of two bodies with different temperatures becomes smaller when the temperature difference increases, and the RCA is always smaller than in the isothermal case.[44] However, if the mechanical behavior of the material is sensitive to temperature changes, the above RCA decrease may be "hidden" by RCA rise due to the reduction in the mechanical characteristics of the material.

Use of the following nondimensional quantities $\tilde{A}=A_r/A_a$; $W=\frac{w}{A_a}\frac{(1-\nu^2)}{E}$; $\tilde{D}=RD\sigma$; $\tilde{\sigma}=\sigma/R$, and designations for the integrals $F_1(h)=\frac{1}{\sqrt{2\pi}}\int_h^\infty(\xi-h)\exp\left[-\xi^2/2\right]d\xi$, $F_{3/2}(h)=\frac{1}{\sqrt{2\pi}}\int_h^\infty(\xi-h)^{3/2}\exp\left[-\xi^2/2\right]d\xi$, eqs. (13) and (14) are rewritten as

$$\tilde{A}=\pi\tilde{D}F_1(h), \tag{15}$$

$$W=\frac{4}{3}\tilde{D}\sqrt{\tilde{\sigma}}\left[F_{3/2}(h)+\frac{3}{2\pi}\frac{\alpha T}{\sqrt{\tilde{\sigma}}}(1+\nu)F_1(h)\right]. \tag{16}$$

These equations describe the dependence of the relative RCA on the nondimensional load in the parametric form. The relative separation h is used as the parameter. For isothermal contact, eq. (16) is written in the form:

$$W_H=\frac{4}{3}\tilde{D}\sqrt{\tilde{\sigma}}F_{3/2}(h). \tag{17}$$

If the rheological behavior is governed by a single relaxation time, the simple exponential dependence describes its temperature-dependent modulus:

$$E=E_0\exp\left[-\beta T\right], \tag{18}$$

where β is a constant having dimension of the reciprocal of the temperature and conventionally termed as the rheological parameter. Substituting modulus (18) in eq. (16) is derived a parametric system of equations, which describes the temperature dependence of the RCA. This system involves eq. (16) and modified eq. (17). The latter is of the form:

$$W_0\exp\left(\beta T\right)=\frac{4}{3}\tilde{D}\sqrt{\tilde{\sigma}}\left[F_{3/2}(h)+\frac{3}{2\pi}\frac{\alpha T}{\sqrt{\tilde{\sigma}}}(1+\nu)F_1(h)\right], \tag{19}$$

where $W_0=W/E_0$.

RESULTS AND DISCUSSION

In general, the main surface features that are used in the interpretation of friction and wear phenomena are the number of local contact spots, the distribution of real areas of contact between the rough surfaces, mean curvature radius of asperities, and root-mean-square (Rq) of asperity peaks (but not Rq of surface height points).[43,45–47] Recently, the new approach is proposed[48] for surface characterization based on the analysis of cumulative distributions of surface area and material volume. In addition to statistical parameters of density of height distribution, such as Sa, Sq, Sku Ssk, for the surface characterization of functional (tribological) properties of surfaces, the following functional characteristics were proposed: bearing projected area, bearing surface area and bearing material volume as functions of height (amplitude) of a surface. These parameters are similar to the bearing area curve (Abbott–Firestone curve that is a cumulative distribution of height points[27]), but differ from it due to their relation to the topographical properties of a surface.

The bearing projected area curve is a cumulative distribution of areas which are material, hit by the cutting plane along the height range from maximum to minimum height point. Thus, the bearing projected area curve has strong relation to the important functional property of an engineered surface as the RCA of rough polymer surfaces.

The bearing surface area curve is a cumulative distribution of areas that is calculated as a sum of surface areas which exceed the cutting plane at given height. This curve is of interest in polymer tribology for calculating the adhesion interaction of rough surfaces. In most of the cases, the adhesion wear is the dominant wear mechanism at nanoscale friction.[49,50] For the achievement of more precise results of the calculation, the surface was represented as a set of triangles that allowed the reconstruction of a rough surface close to its original topography.

The bearing material volume is a cumulative distribution of material volume. Choosing the threshold plane at certain height, the material volume was calculated as a sum of volumes of single truncated right triangular prisms. The bearing material volume is crucial for estimating the functional parameters of polymer surfaces as the volume loss of surface due to wear.

The AFM image of fracture surface of PTFE composites containing 1% of the furnace (carbon black) in Figure 2(a) is shown. Carbon black (CB) is regarded as a group of widely used commercial fillers, which contain nanosized primary particles as well as primary aggregates in different proportion, so they hold a certain promise as a combination filler for improvement of PTFE wear resistance. The role of morphological features of the CB primary aggregates in improving PTFE tribological behavior is now under deep investigation,[51–54] coming to the conclusion that the wear reducing action of carbon black consists in the prevention of extracting the PTFE fiber from the PTFE composite. An example of functional bearing curves mentioned above is shown in Figure 2(b,d) for surface of PTFE composite [see Figure 2(a)]. All bearing curves, which were calculated using data of fracture surface, have a symmetrical shape and fully correspond to the classical behavior of the cumulative distribution for "virgin" (fresh or fracture) surface. The bearing curves of worn surface, for any others materials,[47] have a slightly different shape. To compare the general shape of bearing curves of worn and "virgin" surfaces, one can conclude that all functional bearing curves of worn surfaces haven't a part of curve which is commonly called "peak zone."[28,30] The analysis of the missing "peak zone" of curves can be easy used for a quantitative assessment of wear of polymers tested.

As mentioned in the theoretical section "Contact Problems with Adhesion Interaction," the theories of adhesion contact between sphere and flat surface were formulated by Johnson, Kendall, and Roberts (JKR model) and Deryaguin, Muller, and Toporov (DMT model). Analysis shows that each of these models is true for certain combinations of physical-mechanical and geometric characteristics of the bodies (see Figure 3). The DMT theory is applicable to the materials for which the point with the coordinates (K, γ) lies below the corresponding line plotted at the constant radius of asperity tip R. Here K is the reduced stiffness of the contacting materials and γ is the interface energy.

The former considers the adhesion as a change in surface energy only where the two bodies are in contact (that is, the attractive forces are infinitely short-ranged). Tentative assessment of the

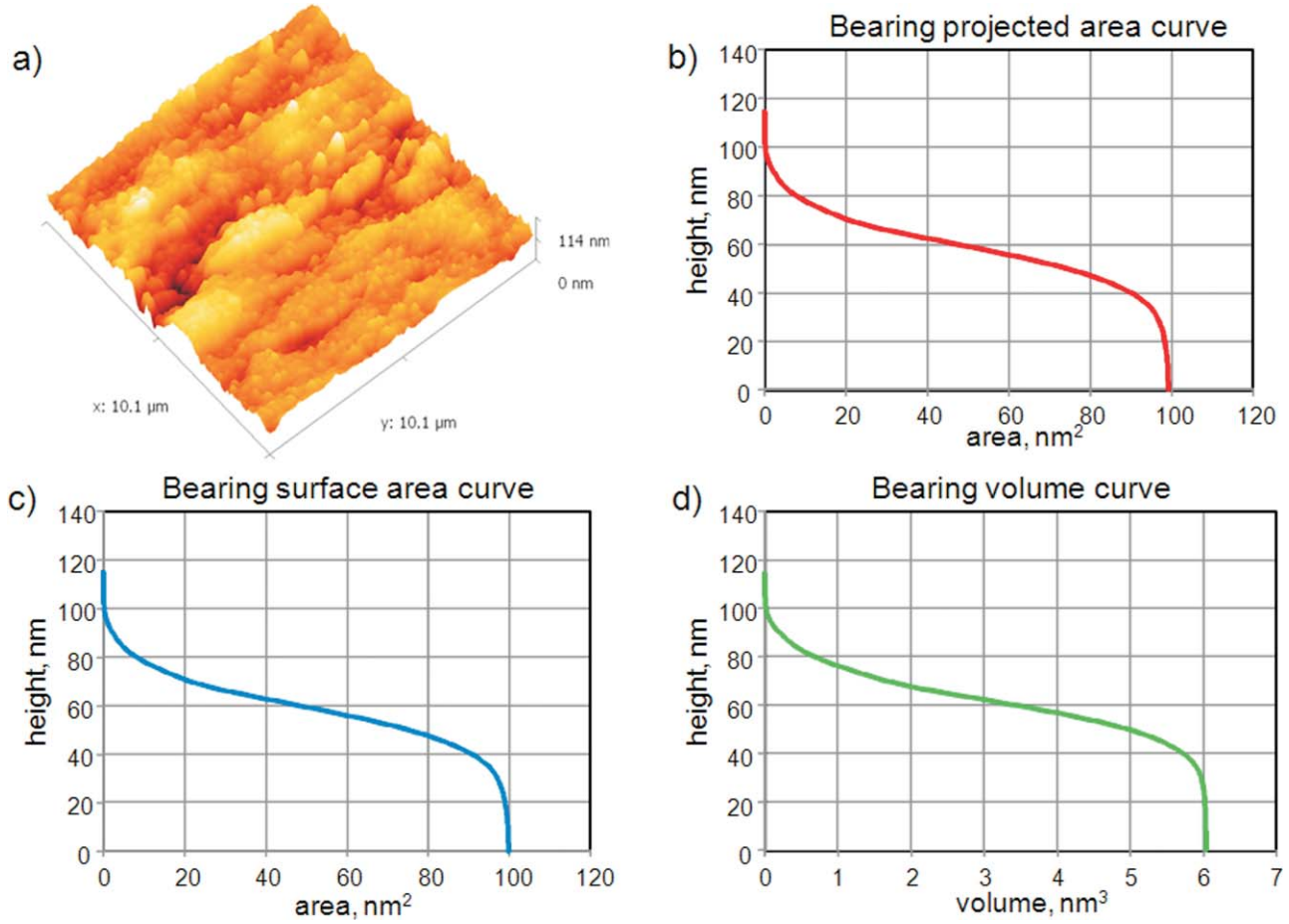

Figure 2. Surface of PTFE composite containing 1% of furnace. (a) AFM image of 5 × 5 μm^2. The main roughness parameters calculated for given AFM image are Ra = 17.26 nm, Rq = 21.96 nm, Rsk = −0.35, Rku = 3.38. (b) The bearing projected area curve of surface PTFE composite showing the distribution of "contact areas" regarding the height. (c) The bearing surface area curve displaying the distribution of surface from maximum to minimum height points. (d) The bearing volume curve of PTFE composite reflects the distribution of material volume. [Color figure can be viewed in the online issue, which is available at wileyonlinelibrary.com.]

effect of intermolecular forces can be made using the adhesion parameter.[55]

$$\Delta_C = \frac{1}{3\sigma}\left(\frac{9\ \pi\ R^2 \Delta\ \gamma}{8E}\right)^{2/3}.$$

Estimation of the adhesion forces shows that the discrete contact is highly sensitive to its adhesion ability.[56] So, larger magnitudes of Δ_C can increase the RCA more than 100 times. The relation $\Delta_C < 0.1$ can occur only in the case when at least one of the contacting bodies is completely elastic. Theoretical and experimental studies have shown that contact is formed by adhesion and surface forces are dominant when $\Delta_C > 0.1$.

Since physical-mechanical properties of mating materials are introduced into eq. (1) in addition to roughness parameter, the condition $\Delta_C \geq 0.1$ can determine the ultimate mean arithmetic

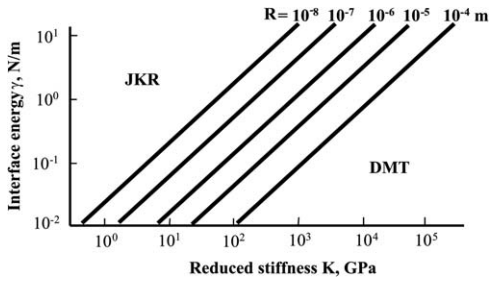

Figure 3. Domains of parameters (K, γ) where either of two models (JKR or DMT) is correct.

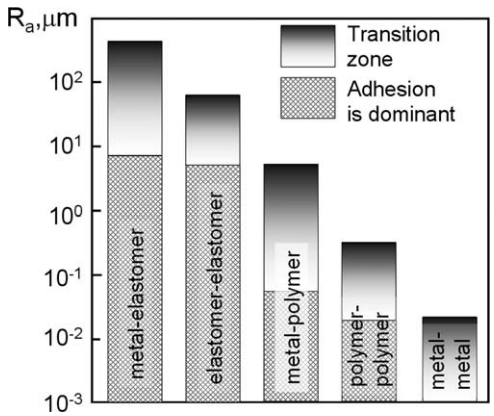

Figure 4. Inter-relation of roughness, mechanical properties, and adhesion in a contact.

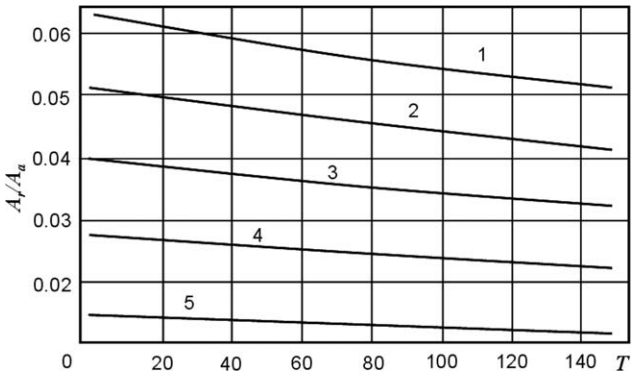

Figure 5. The RCA A_r/A_a versus temperature T at different nondimensional pressure W: $1-W=10$, $2-W=8$, $3-W=6$, $4-W=4$, $5-W=2$.

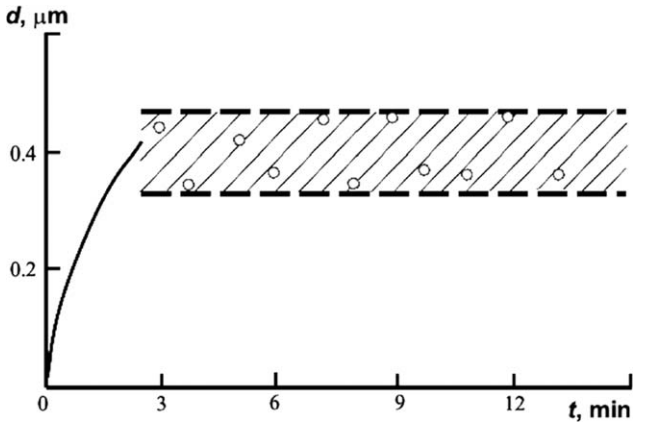

Figure 6. Thickness of transferred film of PTFE as a function of friction duration (load = 0.05 MPa, sliding velocity = 0.35 m/s).

deviations of the equivalent roughness $Ra=(Ra_1+Ra_2)^{1/2}$ below which the degree of adhesion in the contact should be taken into account (see Figure 4). A transition region exists above this level when condition $\Delta_C>0.1$ is fulfilled only at a certain combination of properties of contact materials; hence each specific case needs validation. This analysis indicates that it is impossible to study contact of any materials at nanoscale unless the atomic and molecular interactions between the surfaces are taken into account.

The effect of the excess temperature on the relative RCA is shown in Figure 5. The higher temperature, the smaller RCA becomes. This situation takes place in a sliding contact and the so-called "thermoelastic instability" appears. The heat flow across a contact spot gives rise to expansion of asperity being in contact and its "buckling" as against the isothermal case. A mean size of contact spot and the RCA becomes smaller. To retain the earlier value of RCA, the nominal contact load should be increased.

Thus, it was shown that the RCA of two bodies with different temperatures becomes smaller, if the temperature difference increases. The RCA are always smaller than those in the isothermal case. However, the mechanical behavior of material is sensitive to temperature change (for example, the elastic modulus of most polymers drops with increasing the temperature). In this connection, the way out is considering both factors, the thermal expansion of the bodies in contact and the reduction in the mechanical characteristics with increasing the temperature, in their combined action on the RCA.

Friction transfer attracted a lot of attention in the tribological community generating many new concepts and hypotheses.[57] Polymers are most susceptible to the friction transfer when rubbing both against metals and polymers. As an illustration let us consider friction between PTFE and PE.[10] Experiments were carried on the wear tester with the block-on-ring geometry. It has been found that PTFE is transferred in the form of flakes of very small sizes during the initial period of friction. The thickness of the film transferred increases monotonically and then oscillates around a mean value; the magnitude and amplitude of the oscillations depend on the test conditions, especially on the load and sliding velocity (see Figure 6). Self-lubricating additives such as PTFE are used to optimize the frictional properties of solids.[58,59] It is important that the lubricant is transferred to the surface of the contact material during sliding reducing the interfacial shear stress and friction coefficient.

Figure 7(a) shows the well-known schematic representation of the semi-crystalline nature of PTFE.[60] There are lamellae of crystalline layers with amorphous regions between them. Figure

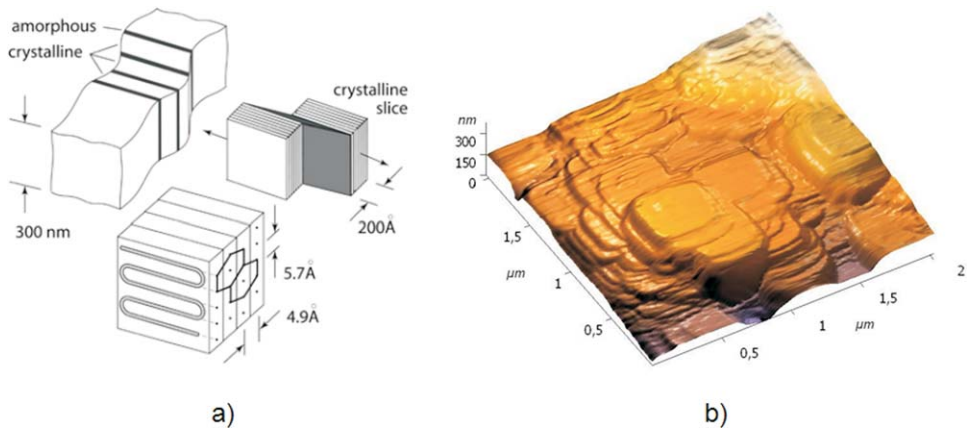

Figure 7. (a) Microstructure of PTFE; (b) AFM-image of PTFE friction surface. [Color figure can be viewed in the online issue, which is available at wileyonlinelibrary.com.]

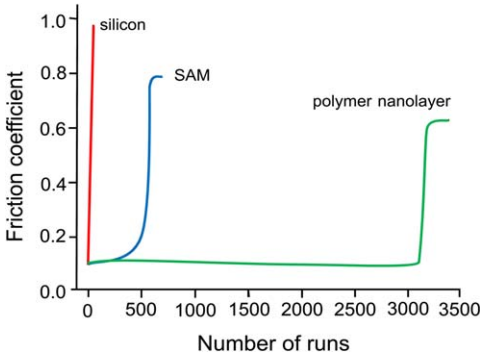

Figure 8. Schematic representation of friction coefficient against steel ball versus a number of reciprocal sliding cycles for silicon, SAM, and triplex nanolayer (after Luzinov and Tsukruk[21–23]). [Color figure can be viewed in the online issue, which is available at wileyonlinelibrary.com.]

7(b) illustrates the AFM image of the PTFE surface after friction tests. Crystallites are clearly seen on the friction surface. They are disordered which proves their free motion occurred during friction. Therefore, the presence of free slices governs the reduction of the friction coefficient and frictional transfer for the materials filled with PTFE.

One more consequence of the polymer transfer is a change in the roughness of both surfaces in contact. The roughness of polymer surface undergo large variation during the unsteady wear until the steady wear is reached, while the roughness of the metal surface is modified due to the transfer of polymer.

Theoretical and experimental studies[21,22,61] have been devoted to polymer ultrathin layers (such as poly[styrene-*b*-butadiene] (SB), poly[styrene-*b*-butadiene-*b*-styrene] (SBS), and poly[styrene-*b*-(ethylene-*co*-butylene)-*b*-styrene] (SEBS)) made of block copolymers due to their potential applications in many technological areas, including coatings, nanolithography, microelectronics, lubricants, adhesives, and membrane separation. These films self-organize in a variety of ordered microdomain structures from spherical to lamellar as the fraction and molar mass of the blocks constituting the copolymers are changed. The formation of the microdomain structure within SEBS layers is completely suppressed only at extremely small thicknesses below 3 nm. In this case, the layers are completely structureless but still dense, complete and chemically tethered. At this very small thickness (well below the diameter of the macromolecular chain, which is equal to 12.3 nm), the layers display somewhat disordered surface morphology.

The wear resistance of the triplex coatings was tested under conditions of the mesoscale shearing contact (contact radius, ~10 μm). This involved the contact of a steel ball and local pressures/velocities comparable with that of conventional MEMS operating conditions. In this method of wear testing, a sharp increase of the friction forces indicates detrimental surface failure. Experimental data are shown for the trilayer surface structures in comparison with a bare silicon surface, and the grafted rubber interlayer (see Figure 8). During the test, the local pressure reached 1.2 GPa, which was much higher than the yield strength of a vast majority of polymeric materials. Under these severe loading conditions, the wear resistance mechanism was controlled by the ability of the surface to self-heal and restore itself, rather than by direct elastic resistance of the surface. Indeed, all reference surfaces failed almost immediately (Figure 8). Alkylsilane SAM failed after 900 cycles. The trilayer surface structure showed much higher wear stability, and was worn down after 3000–3500 cycles due to the intensive thermo-oxidation occurring in the contact area.

CONCLUSIONS

A widespread interest in plastics has grown in the mid twentieth century due to the features of their structure, specific mechanical behavior, and considerable possibility to change the polymer properties. But creep behavior of polymers (strong dependence of their properties on temperature), low heat conductivity, and sensitivity to the environment often posed numerous problems. Extensive studies over many years have developed the field of modern engineering in which the plastics can be applied as tribological materials, more commonly in the form of coatings and solid lubricants. The latter are used either in the pure form or as the composites or laminated structures. Thin polymer films, e.g., self-assembled monolayers formed by the chemisorption and physisorption of organic molecules (polymers) are prospective boundary lubricants in the fast-growing area of the memory storage devices, the microelectromechanical systems and other precision mechanisms.

Further progress in the field of friction and wear of polymers and their composites should be based on solving a number of important problems which will allow to establish more refined mechanisms which occur in the working surfaces of friction pairs. It appears important to study the structural changes at molecular level in the surface layers, and to investigate the tribo-chemical reactions.

ACKNOWLEDGMENTS

This work was partially funded through the European Metrology Research Programme (EMRP) Project IND11 MADES. The EMRP is jointly funded by the EMRP participating countries within EURAMET and the European Union. The authors thank Dr. Dai and Dr. Bosse from Physikalisch-Technische Bundesanstalt (PTB, Germany) for collaboration and fruitful discussion about surface characterization.

REFERENCES

1. Myshkin, N.; Kovalev, A. In Polymer Tribology; Sinha, S.; Briscoe, B., Eds.; Imperial College London: London, **2009**, Chapter 1, pp 3–37.
2. Myshkin, N. K.; Petrokovets, M. I.; Kovalev, A. *Tribol. Int.* **2005**, *38*, 910.
3. Brostow, W.; Kovacevic, V.; Vrsaljko, D.; Whitworth, J. *J. Mater. Educ.* **2010**, *32*, 273.
4. Brostow, W. *Pure Appl. Chem.* **2009**, *81*, 417.
5. Wieleba, W. *Arch. Civ. Mech. Eng.* **2007**, *7*, 185.
6. Adhikari, R.; Brostow, W.; Datashvili, T.; Henning, S.; Menard, B.; Menard, K. P.; Michler, G. H. *Mater. Res. Innov.* **2012**, *16*, 19.

7. Brostow, W.; Brozynski, M.; Datashvili, T.; Olea-Mejia, O. *Polym. Bull.* **2011**, *67*, 1671.
8. Brostow, W.; Kumar, P.; Vrsaljko, D.; Whitworth, J. *J. Nanosci. Nanotechnol.* **2011**, *11*, 3922.
9. Bahadur, S. *Wear* **2000**, *245*, 92.
10. Bely, V. A.; Sviridenok, A. I.; Petrokovets, M. I.; Savkin, V. G. Friction and Wear in Polymer Based Materials; Pergamon Press: Oxford, **1982**.
11. Friedrich, K.; Schlarb, A. K. Tribology of Polymeric Nanocomposites: Friction and Wear of Bulk Materials and Coatings. Elsevier Science: Amsterdam, **2008**.
12. Chang, L.; Zhang, Z.; Ye, L.; Friedrich, K. *Wear* **2007**, *262*, 699.
13. Samyn, P.; Schoukens, G.; Verpoort, F.; van Craenenbroeck, J.; de Baets, P. *Macromol. Mater. Eng.* **2007**, *292*, 523.
14. Zhang, G.; Yu, H.; Zhang, C.; Liao, H.; Coddet, C. *Acta Mater.* **2008**, *56*, 2182.
15. Leaderman, H. *Text. Res. J.* **1941**, *11*, 171.
16. Kaltzakorta, O.; Wäsche, R.; Hartelt, M.; Aginagalde, A.; Tato, W. *Tribol. Lett.* **2012**, *48*, 209.
17. Makinson, K. R.; Tabor, D. P. *Roy. Soc. A-Math. Phys.* **1964**, *281*, 49.
18. Pooley, C. M.; Tabor, D. *Nature* **1972**, *237*, 88.
19. Renouf, M.; Cao, H.-P.; Nhu, V.-H. *Tribol. Int.* **2011**, *44*, 417.
20. Panin, S.; Kornienko, L.; Wannasri, S.; Piriyaon, S.; Poowadin, T.; Ivanova, L.; Shil'ko, S.; Sergeev, V. *Mech. Comp. Mater.* **2011**, *47*, 513.
21. Luzinov, I.; Julthongpiput, D.; Bloom, P. D.; Sheares, V. V.; Tsukruk, V. V. *Macromol. Symp.* **2001**, *167*, 227.
22. Luzinov, I.; Tsukruk, V. V. *Macromolecules* **2002**, *35*, 5963.
23. Kovalev, A.; Tsukruk, V. In Encyclopedia of Tribology; Wang, Q. J., Chung Y.-W., Eds.; Springer: US, **2013**; pp 2602–2607.
24. Myshkin, N. K.; Petrokovets, M. I. In Mechanical Tribology: Materials, Characterization, and Applications; Totten, G.; Liang, H., Eds.; Marcel Dekker: New York, **2004**; Chapter 3, pp 57–94.
25. Johnson, K. L.; Kendall, K.; Roberts, A. D. P. *Roy. Soc. A-Math. Phys.* **1971**, *324*, 301.
26. Derjaguin, B.; Muller, B.; Toporov, Y. *J. Colloid Interf. Sci.* **1975**, *53*, 314.
27. Abbott, E. J.; Firestone, F. A. *Mech. Eng.* **1933**, *59*, 569.
28. DIN 4776. Kenngrößen Rk, Rpk, Rvk, Mr1, Mr2 zur Beschreibug des Materialanteils im Rauheitsprofil—Meßbedingungen und Auswerteverfahren; In Deutsche Norm; Beuth Verlag GmbH: Berlin, **1990**.
29. ISO 13565. Geometrical Product Specifications (GPS)—Surface texture: Profile Method Surfaces Having Stratified Functional Properties; AFNOR: Paris, **1998**.
30. Jiang, X.; Scott, P. J.; Whitehouse, D. J.; Blunt, L. P. *Roy. Soc. A-Math. Phys.* **2007**, *463*, 2071.
31. Jiang, X.; Scott, P. J.; Whitehouse, D. J.; Blunt, L. P. *Roy. Soc. A-Math. Phys.* **2007**, *463*, 2049.
32. Whitehouse, D. Surfaces and Their Measurement; Kogan Page Science: London, **2002**.
33. Sayles, R. S.; Thomas, T. R. *Nature* **1978**, *271*, 431.
34. Gadelmawla, E. S.; Koura, M. M.; Maksoud, T. M. A.; Elewa, I.; Soliman, H. H. *J. Mater. Process. Tech.* **2002**, *123*, 133.
35. Whitehouse, D. J. Handbook of Surface and Nanometrology; CRC Press: New York, **2011**.
36. Thomas, T. R. Rough Surfaces; Imperial College Press: London, **1999**.
37. Sedlaček, M.; Podgornik, B.; Vižintin, J. *Tribol. Int.* **2012**, *48*, 102.
38. Corral, I. B.; Calvet, J. V.; Salcedo, M. C. *Int. J. Mach. Tool Manu.* **2010**, *50*, 621.
39. Poon, C. Y.; Sayles, R. S. *J. Phys. D Appl. Phys.* **1992**, *25*, A249.
40. Myshkin, N.; Petrokovets, M.; Chizhik, S. *Tribol. Int.* **1998**, *31*, 79.
41. Myshkin, N.; Kovalev, A.; Makhovskaya, Y.; Torskaya, E.; Goryacheva, I. *Tribology* **2010**, *4*, 130.
42. Quaglini, V.; Dubini, P.; Ferroni, D.; Poggi, C. *Mater. Des.* **2009**, *30*, 1650.
43. Greenwood, J. A.; Williamson, J. B. P. P. *Roy. Soc. A-Math. Phys.* **1966**, *295*, 300.
44. Petrokovets, M. I. *J. Frict. Wear* **1999**, *20*, 1.
45. Greenwood, J. A. *Br. J. Appl. Phys.* **1966**, *17*, 1621.
46. Archard, J. F. *J. Appl. Phys.* **1953**, *24*, 981.
47. Archard, J. F. P. *Roy. Soc. A-Math. Phys.* **1957**, *243*, 190.
48. Dai, G.; Pohlenz, F.; Bosse, H.; Kovalev, A.; Spaltmann, D.; Woydt, M. In Proceedings of the 13th international conference of the **EUSPEN**, Berlin, Germany, May 27–31, **2013**; Leach, R.; Shore, P., Eds.; EUSPEN Headquarters: Bedford, 2013.
49. Jacobs, T. D. B.; Carpick, R. W. *Nat. Nanotechnol.* **2013**, *8*, 108.
50. Mo, Y.; Turner, K. T.; Szlufarska, I. *Nature* **2009**, *457*, 1116.
51. Goyal, R. K.; Yadav, M. *J. Appl. Polym. Sci.* **2013**, *127*, 3186.
52. Aderikha, V. N.; Shapovalov, V. A.; Pleskachevskii, Y. M. *J. Frict. Wear* **2008**, *29*, 120.
53. Aderikha, V. N.; Shapovalov, V. A. *Wear* **2010**, *268*, 1455.
54. Takeichi, Y.; Wibowo, A.; Kawamura, M.; Uemura, M. *Wear* **2008**, *264*, 308.
55. Fuller, K. N. G.; Tabor, D. P. *Roy. Soc. A-Math. Phys.* **1975**, *345*, 327.
56. Myshkin, N.; Petrokovets, M.; Chizhik, S. *Tribol. Int.* **1999**, *32*, 379.
57. Myshkin, N. K. *Wear* **2000**, *245*, 116.
58. Yang, X.-B.; Jin, X.-Q.; Du, Z.-M.; Cui, T.-S.; Yang, S.-K. *Ind. Lubr. Tribol.* **2009**, *61*, 254.
59. Karnath, M. A.; Sheng, Q.; White, A. J.; Mueftue, S. *Tribol. T.* **2011**, *54*, 36.
60. Schadler, L. S.; Brinson, L. C.; Sawyer, W. G. *JOM-J. Min. Met. Mat. S.* **2007**, *59*, 53.
61. Iyer, K. S.; Luzinov, I. *Langmuir* **2003**, *19*, 118.